Proc. Natl. Acad. Sci. USA
Vol. 93, pp. 2403–2407, March 1996
Neurobiology

Mice deficient for prion protein exhibit normal neuronal excitability and synaptic transmission in the hippocampus

(prion protein gene knockout mice/γ-aminobutyric acid/long-term potentiation/synaptic plasticity)

PIERRE-MARIE LLEDO*, PATRICK TREMBLAY†, STEPHEN J. DEARMOND‡, STANLEY B. PRUSINER†§, AND ROGER A. NICOLL*¶

Departments of *Cellular and Molecular Pharmacology and Physiology, ‡Pathology, †Neurology, §Biochemistry and Biophysics, University of California, San Francisco, CA 94143

Contributed by Roger A. Nicoll, December 1, 1995

ABSTRACT **We recorded in the CA1 region from hippocampal slices of prion protein (PrP) gene knockout mice to investigate whether the loss of the normal form of prion protein (PrP^C) affects neuronal excitability as well as synaptic transmission in the central nervous system. No deficit in synaptic inhibition was found using field potential recordings because (*i*) responses induced by stimulation in stratum radiatum consisted of a single population spike in PrP gene knockout mice similar to that recorded from control mice and (*ii*) the plot of field excitatory postsynaptic potential slope versus the population spike amplitude showed no difference between the two groups of mice. Intracellular recordings also failed to detect any difference in cell excitability and the reversal potential for inhibitory postsynaptic potentials. Analysis of the kinetics of inhibitory postsynaptic current revealed no modification. Finally, we examined whether synaptic plasticity was altered and found no difference in long-term potentiation between control and PrP gene knockout mice. On the basis of our findings, we propose that the loss of the normal form of prion protein does not alter the physiology of the CA1 region of the hippocampus.**

Scrapie and bovine spongiform encephalopathy of animals as well as Creutzfeldt–Jakob disease of humans are neurodegenerative disorders caused by prions (1, 2). During the disease process, the cellular isoform of prion protein (PrP^C) is post-translationally modified to an abnormal or scrapie isoform designated as PrP^{Sc} (3–5). A wealth of data indicates that PrP^{Sc} is required for the transmission and pathogenesis of the prion diseases (6–9). In contrast, the physiological function of the normal host protein PrP^C remains obscure, although elucidating its function might help explain the pathogenesis of prion diseases (for review, see ref. 10). The PrP gene was disrupted by homologous recombination, and homozygous PrP gene knockout mice ($Prnp^{0/0}$) were found to develop normally (11). In addition, histologic and behavioral studies failed to show any abnormalities. However, it has been recently reported that hippocampal slices from $Prnp^{0/0}$ mice have defects in γ-aminobutyric acid type A ($GABA_A$) receptor-mediated synaptic inhibition and long-term potentiation (LTP) (12–14). These findings seemed of considerable importance, not only in providing clues to the physiological role of PrP^C and elucidating the pathological changes that underlie the epileptiform activity seen in Creutzfeldt–Jakob disease but because they would make difficult the use of antisense oligonucleotides as a therapeutic strategy for combating the lethal prion diseases. We therefore compared a number of properties involved in the control of neuronal excitability in slices of the hippocampus CA1 region in $Prnp^{0/0}$ mice and in normal mice but found no difference between the two groups. These results are consistent with the hypothesis that the etiology of prion diseases is independent of the loss of the normal form of prion protein (9, 15).

The publication costs of this article were defrayed in part by page charge payment. This article must therefore be hereby marked "*advertisement*" in accordance with 18 U.S.C. §1734 solely to indicate this fact.

MATERIALS AND METHODS

The embryonic stem cells used for homologous recombination were from 129/Sv mice (16, 17). A mosaic male mouse generated from introduction of the embryonic stem cells into the blastocyst was mated with female C57BL/6 mice to produce $Prnp^{0/+}$ mice (11). These $Prnp^{0/+}$ mice were mated to each other to produce $Prnp^{0/0}$ and $Prnp^{+/+}$ animals (designated group I). These two strains were maintained by intercrossing through several generations. In parallel, the genetic background of the Prnp-ablated animals was modified by crossing the $Prnp^{0/+}$ mice with wild-type FVB animals for two and four generations before brother-to-sister matings were done to obtain FVB.$Prnp^{0/0}$ N2F1 and FVB.$Prnp^{0/0}$N4F1 (designated group II and III, respectively). Genotype of PrP gene knockout mice was checked by PCR analysis of tail DNA (8). Our studies were carried out "blind," and the code was broken only after data analysis was completed for a given set of experiments; data generated independently from the three experimental groups were analyzed separately before being pooled.

Standard procedures for preparing and maintaining hippocampal slices were used as described (18). Slices (400 μm thick) were allowed to recover for at least 1 hr and then transferred individually to a submersion recording chamber where they were superfused at room temperature with artificial cerebrospinal fluid (119 mM NaCl, 2.5 mM KCl, 2.5 mM $CaCl_2$, 1.3 mM $MgSO_4$, 26 mM $NaHCO_3$, 1 mM NaH_2PO_4, 10 mM D-glucose) and equilibrated with 95% O_2/5% CO_2.

Extracellular field recordings were made from 8-mo-old mice with glass electrodes containing 1 M NaCl (impedance of 5–20 MΩ) using an Axoclamp-2A amplifier (Axon Instruments, Burlingame, CA). To evoke synaptic responses, stimuli (100-μs duration at a frequency of 0.05 to 0.1 Hz) were delivered through fine bipolar stainless steel electrodes placed in stratum radiatum. Field responses were filtered at 1 kHz, digitized at 4 kHz on a TL-1 interface (Axon Instruments), and collected on a 486 IBM compatible computer. A modification of PCLAMP software was used for all analysis. The relationships between field excitatory postsynaptic potential (fEPSP) slopes and population spike amplitudes (E–S relationships) were constructed by delivering ascending series of stimulus inten-

Abbreviations: PrP, prion protein; PrP^C, cellular isoform of PrP; PrP^{Sc}, scrapie isoform of PrP; $Prnp^{0/0}$, homozygous PrP gene knockout mice; LTP, long-term potentiation; fEPSP, field excitatory postsynaptic potential; IPSP, inhibitory postsynaptic potential; E–S relationship, relationship between fEPSP slopes and population spike amplitudes; IPSC, inhibitory postsynaptic currents; $GABA_A$, γ-aminobutyric acid type A.

¶To whom reprint requests should be addressed.

sities. The population spike amplitude of the evoked responses was measured between the negative peak and a line drawn on the top of the two positive peaks, whereas for the negative population EPSP, the slope was measured within the first millisecond. So that data from different slices could be compared, the E–S relationship was normalized by expressing both field EPSP slopes and the related population spike amplitudes as values relative to their thresholds (arbitrarily set at 0.1 and 10 for the population spike amplitude and the field EPSP slope, respectively). Normalized E–S curves were fitted with a sigmoidal function: $S = S_{max}/(1 + \exp[(E_{50} - E)/k)]$ where S_{max} is the maximal amplitude of the normalized population spike amplitude, E_{50} is the value of fEPSP slope at which the amplitude of population spike reaches half of its maximum value, and k is inversely proportional to the steepness of the function. For LTP experiments, baseline transmission was monitored at 0.05 Hz, and groups of three potentials were averaged to yield one measurement per minute of the initial slope of the fEPSP. The initial values of EPSP were adjusted to about half-maximal. The LTP-inducing stimulus consisted of one train of 100 stimuli at 100 Hz after 10 min of stable baseline in the presence of 30 μM bicuculline methiodide and with CA3 removed by a surgical cut.

Intracellular recordings using sharp microelectrodes were performed to measure intrinsic membrane properties, neuronal excitability, and the reversal potential for inhibitory postsynaptic potentials (IPSPs) in CA1 neurons. Eight-week-old and 8-mo-old mice were used for these experiments. Monosynaptic fast, bicuculline-sensitive IPSPs were evoked by stimulating close to the CA1 pyramidal cell layer, and neurons of the CA1 region were recorded in bridge mode with sharp microelectrodes containing 4 M potassium acetate and 50 mM QX-314 (50–80 MΩ). Signals were amplified (Axoclamp-2A, Axon Instruments), displayed on an oscilloscope and chart recorder, and stored on digital tape recorder [DTR 1204, Biologic (Grenoble, France), sampling frequency 48 kHz]. $GABA_A$-mediated IPSPs were pharmacologically isolated using artificial cerebrospinal fluid containing 20 μM 6-cyano-7-nitroquinoxaline-2,3-dione (CNQX), 50 μM D-2-amino-5-phosphonovalerate (D-APV) and 500 μM CGP-35348 to block EPSPs and $GABA_B$ IPSPs. During current-clamp recordings, several criteria were used to select cells for analysis: (*i*) changes in resting membrane potential not exceeding 5 mV; and (*ii*) no sudden drop in the input resistance and constant amplitude of the spike obtained by direct activation of the neuron before diffusion of QX-314 into the cell. Measurements of fast IPSPs were made ≈20 msec after the stimulus artifact, and the IPSP reversal potential was determined by altering the membrane potential with DC holding current.

Whole-cell, patch-clamp recordings were made on CA1 pyramidal neurons obtained from 3-week-old mice. Patch pipettes (5 MΩ) pulled from borosilicate glass contained 123 mM cesium gluconate, 10 mM CsCl, 10 mM Hepes, 10 mM Cs-EGTA, 8 mM NaCl, 1 mM $CaCl_2$, 2 mM Mg-ATP, 0.3 mM GTP, 0.2 mM cAMP, and 10 mM D-glucose (pH 7.3, 290 mosM). Slices were perfused with the same bath solution described for current-clamp recordings giving a calculated Cl^- equilibrium potential of −46 mV. Ionic currents measured by the amplifier (Axopatch 1D, Axon Instruments) were initially recorded on a digital tape recorder after filtering at 2 kHz and were later sampled at 10 kHz. For analysis of kinetic parameters, spontaneous events were detected when the difference between successive data points exceeded a threshold of 5 pA while events having inflections in the rising phase were rejected. This threshold was ≈2.5 times greater than the baseline root-mean-square noise. Stimulus-evoked inhibitory postsynaptic currents (IPSCs) were accepted for analysis when no spontaneous synaptic activity was detected that could interfere with the measured time course. These spontaneously occurring events were blocked by bath application of bicuculline (5 μM) and were therefore spontaneous IPSCs mediated by the activation of $GABA_A$ receptors. Series and input resistances were monitored throughout each experiment with a −3 mV calibration pulse given at a 0.1-Hz frequency and were typically in the range of 10–20 MΩ and 150–200 MΩ, respectively. Experiments were stopped when the series resistance was >20 MΩ or if the series resistance changed >20% during an experiment. All recordings were done at room temperature (22–25°C) and made "blind" to mice genotype. Drugs used were bicuculline methiodide (Sigma); CNQX and D-APV (Tocris Neuramin, Bristol, U.K.); CGP-35348 and QX-314 [from CIBA–Geigy and Astra Pharmaceutical (Worcester, MA), respectively]. Unless otherwise stated, values given in the text are means ± SEMs.

RESULTS AND DISCUSSION

Standard electrophysiological techniques were used to study the excitability of hippocampal slices (18). Initially, we used field potential recordings to assess the level of synaptic inhibition. Under normal conditions pyramidal cells fire a single synchronous population spike in response to stimulation of excitatory synapses in stratum radiatum, whereas when inhibition is compromised, multiple population spikes occur. Responses from $Prnp^{0/0}$ mice (from group I and II) consisted of a single population spike that was indistinguishable from that recorded from normal mice, whereas multiple population spikes were seen only when the $GABA_A$-receptor antagonist

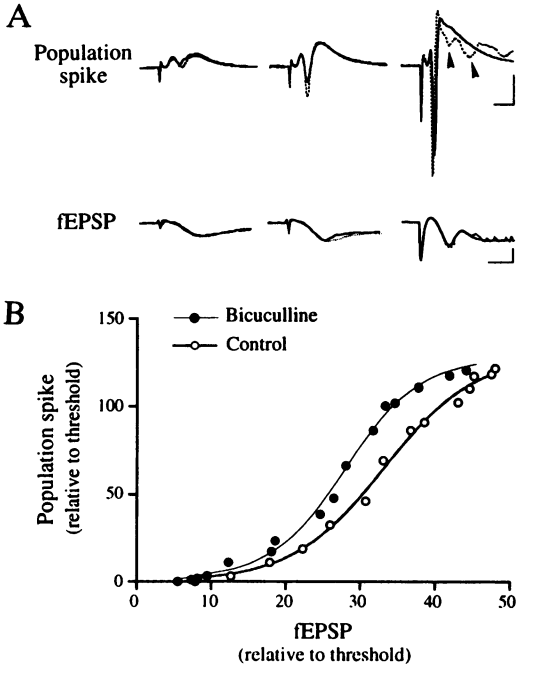

FIG. 1. Field potential recordings fail to reveal a defect in synaptic inhibition in hippocampal slices from $Prnp^{0/0}$ mice. (*A*) Extracellular responses evoked by afferent stimulation in the stratum radiatum were simultaneously recorded in the CA1 pyramidal cell layer to monitor somatic activity (population spikes, upper traces) and in stratum radiatum to record fEPSPs (lower traces). Note the presence of multiple spiking (arrowheads), which were only seen at the higher stimulus strengths and in the presence of 2 μM bicuculline methiodide (dotted traces). Each voltage trace is an average of five consecutive responses evoked at 10-sec intervals. (*B*) The relationship between normalized fEPSP slopes and normalized population spike amplitudes (E–S relationship) recorded extracellularly from a representative experiment illustrates the effect of 2 μM bicuculline on a PrP-null slice (plot from data partially shown in *A*). The E_{50} value from this function shifted from 33 to 27 after bicuculline application. (Bars = upper traces, 1 mV and 10 msec; lower traces, 0.4 mV and 5 msec.)

Table 1. Electrophysiological properties of CA1 pyramidal cells

Variable	Wild type	$Prnp^{0/0}$
r.m.p., mV	−69 ± 4 (13)	−72 ± 5 (11)
Input resistance, MΩ	−95 ± 12 (13)	−83 ± 16 (10)
Membrane time constant, msec	21.4 ± 5.2 (13)	23.3 ± 7.7 (10)
Action potential amplitude, mV	57 ± 5 (5)	60 ± 6 (7)
Action potential duration, msec	2.2 ± 0.4 (4)	2.3 ± 0.5 (3)
Threshold action potential, mV	−59 ± 5 (4)	−57 ± 4 (5)

The resting membrane potential (r.m.p.) was calculated by subtracting the extracellular voltage measured when the electrode was withdrawn from the recorded cell from the resting intracellular voltage. Membrane time constant and input resistance were determined by injecting the cell with 0.1- to 0.3-nA, 500-msec hyperpolarizing current pulses and measuring resultant membrane potential deflections. The membrane time constant was measured from the fitting of a single exponential. Action potential duration was measured as the time between the onset and offset of the action potential. Action potential duration and amplitude were measured from responses to 200-msec depolarizing current pulses. Values are expressed as means ± SEM; number of cells are in parentheses.

bicuculline methiodide (2 μM) was added to the bath (Fig. 1*A*). This finding contrasts with previous findings (12) in which multiple population spikes were recorded in $Prnp^{0/0}$ mice. To measure inhibition and the excitability of pyramidal cells more accurately, we constructed input–output curves by plotting size of the dendritic population excitatory postsynaptic potential (EPSP) versus size of the population spike recorded at the cell body layer for a series of stimulus strengths (E–S relationship; see Fig. 1*B*). We have compared input–output curves in normal and $Prnp^{0/0}$ mice (using group I and II) by measuring the value of normalized fEPSP slope needed to produce 50% of the maximal population spike amplitude (E_{50}) and k, a parameter inversely proportional to steepness of the curve. These values were, respectively, 33.6 ± 2.1 and 6.1 ± 0.7 for control slices (n = 19 from four mice) and 31.4 ± 2.9 and 5.9 ± 0.8 for $Prnp^{0/0}$ slices (n = 12 from four mice). There was no significant difference between the two sets of data ($P > 0.5$, Student's unpaired t test). Moreover, as shown in Fig. 1*B*, partial blockade of synaptic inhibition in a $Prnp^{0/0}$ slice by a low concentration of bicuculline methiodide (2 μM) caused a leftward shift in the curve and the magnitude of the shift in the E_{50} (6.2 ± 1.5; n = 4 from three mice) was not different from the wild type (6.7 ± 1.6; n = 4 from three mice; $P > 0.5$, Student's unpaired t test).

It is noteworthy that the coupling between fEPSP and amplitude of population spike is also strongly influenced by postsynaptic membrane properties such as the resting membrane potential and threshold for spike generation. However, while our input–output experiments should be a sensitive measure of a number of factors that control the postsynaptic excitability of pyramidal cells, we turned to intracellular recordings using sharp electrodes to analyze these factors more directly. As illustrated in Table 1, our intracellular recordings failed to detect any difference in resting membrane potential, input resistance, membrane time constant or firing properties measured in CA1 neurons from $Prnp^{0/0}$ mice (group I and II). We next measured the reversal potential for IPSPs recorded from pyramidal cells using sharp microelectrodes filled with potassium acetate (whole-cell recording could not be used for these experiments because in this case the reversal potential is determined by the anion composition of the pipette solution). Stimulation near the recording site reliably elicited IPSPs in all pyramidal cells. The voltage–current relation of the monosynaptic fast IPSP was established by shifting the membrane potential from around −110 to −50 mV (Fig. 2). Contrary to a previous single electrode voltage-clamp study in which the reversal potential (E_{IPSP}) was shifted by ≈10 mV in the depolarizing direction in $Prnp^{0/0}$ mice (12), we were unable to see any difference in the reversal potential between the two groups of 8-week-old mice (group III) [E_{IPSP} = −70.1 ± 1.9 mV in two control mice (n = 10) and −69.5 ± 2.3 mV in two $Prnp^{0/0}$ mice (n = 8); $P > 0.5$, Student's unpaired t test]. It has been reported that the reversal potential of IPSPs can differ at different stages of development (19, 20); therefore, one possibility that could explain the discrepancy between our results and those from others (12, 13) is the age of the animals. The age of the mice used in the latter study was not specified, and so we also carried out a study with older animals. The values that we obtained from 8-mo-old animals (group I) did not differ from one another or from the values obtained in younger animals [E_{IPSP} = −69.5 ± 2.1 mV (n = 5) in the control slices (two mice) and −70.1 ± 1.9 mV (n = 6) in the $Prnp^{0/0}$ slices from two mice; $P > 0.5$, Student's unpaired t test]. Thus, our intracellular results confirm the extracellular recordings showing that cell excitability as well as the level of synaptic inhibition are unchanged in $Prnp^{0/0}$ mice. Although our experiments on the reversal potential for IPSPs were done with current-clamp recordings, whereas others (12, 13) were done with single electrode voltage-clamp, it seems quite unlikely that this could account for the discrepancy between our studies and those of other investigators. It should be pointed out that in the studies of these other investigators (12, 13), they elicited extremely large inhibitory inputs (up to 5 nA) compared to

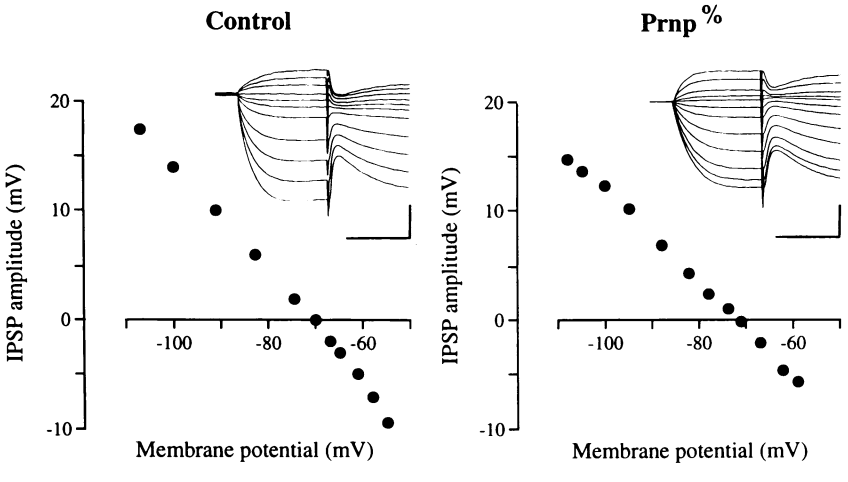

FIG. 2. Reversal potential for monosynaptic fast IPSPs recorded from CA1 neurons is the same between the two $Prnp^{0/0}$ and control animals (group I). A pyramidal cell recorded from a wild-type mouse (*Left*) or from a $Prnp^{0/0}$ mouse (*Right*) was transiently depolarized or hyperpolarized to various membrane potentials while constant low-intensity stimulus was delivered at each potential. Plot of peak amplitude of the evoked fast IPSP against holding potential reveals similar reversal potentials in the two groups. (*Inset* bars = 20 mV and 100 msec.)

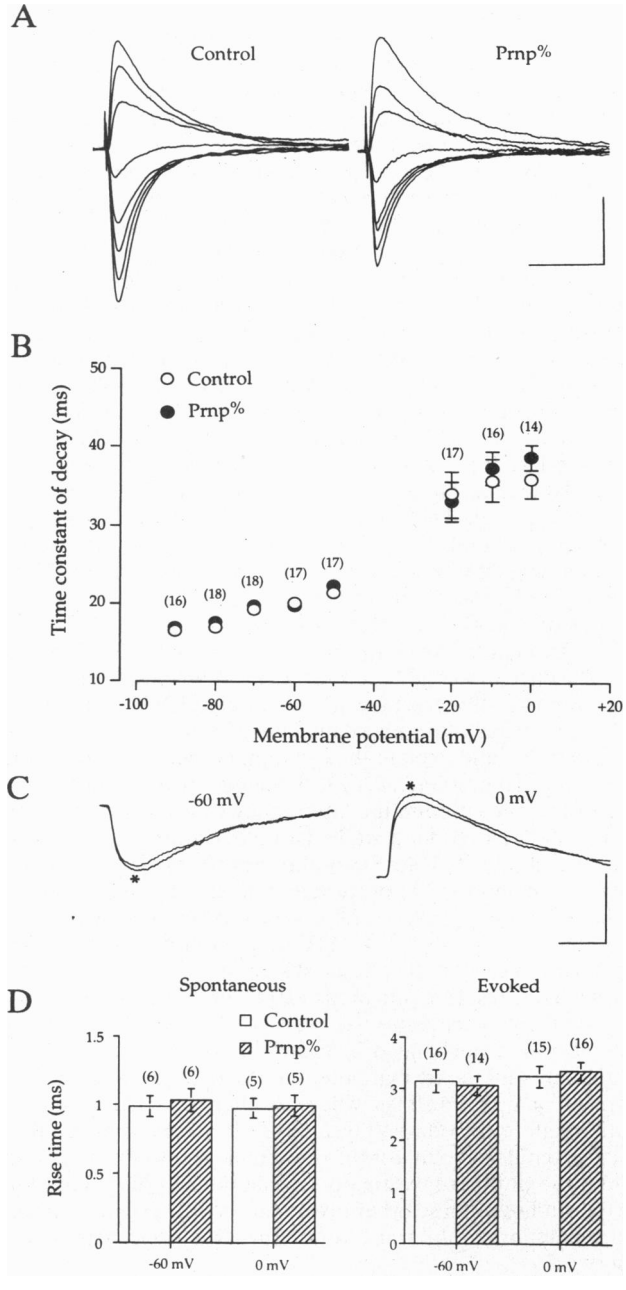

FIG. 3. Kinetics of evoked and spontaneous IPSCs recorded from voltage-clamped CA1 neurons are indistinguishable between 3-week-old control ($n = 4$) and $Prnp^{0/0}$ mice ($n = 4$). Evoked $GABA_A$-induced responses were elicited at holding potentials ranging from −90 to +10 mV (*A* and *B*), whereas spontaneous IPSCs were recorded at −60 and 0 mV (*C* and *D*) with cesium gluconate-containing pipettes using the "blind" recording technique (21). (*A*) Superimposed evoked IPSCs exhibited similar kinetics between neurons from a wild-type mice (Control) or from a $Prnp^{0/0}$ mouse (group II). (*B*) Relationship between decay time constant of evoked IPSCs and holding membrane potential reveals no difference in $Prnp^{0/0}$ neurons compared to control. In all cases, the decay phase of evoked responses was well-fitted with a single exponential. (*C*) The shape of superimposed spontaneous IPSCs recorded at the indicated membrane potentials was similar between the $Prnp^{0/0}$ (*) and control slices. (*D*) Comparison of 10–90% rise times of spontaneous and evoked IPSCs shows no difference between both mouse types. Bars represent means ± SDs; numbers of recorded neurons are indicated in parentheses. (Bars = *A*, 200 pA and 50 msec; *C*, 50 pA and 10 msec.)

ours, which would be equivalent to a few hundred pA, suggesting a more localized synaptic input than in our experiments. Moreover, they reported that in parallel to a depolar-

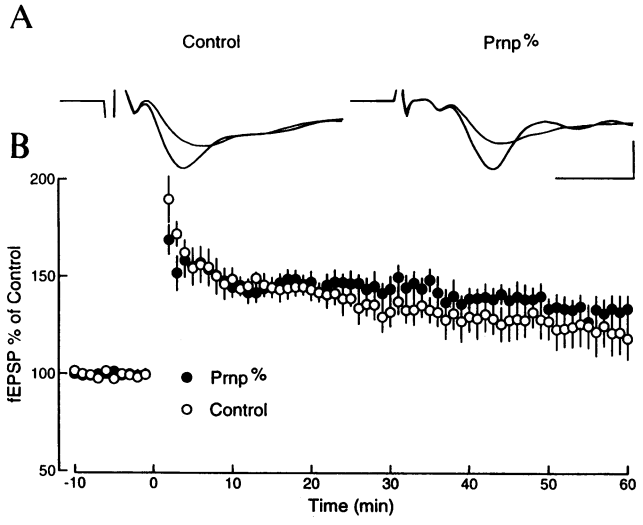

FIG. 4. LTP is normal in the CA1 region of hippocampus from $Prnp^{0/0}$ mice. (*A*) Superimposed fEPSPs recorded before and 40 min after the stimulus train. Each record is the average of 10 traces. (*B*) Plot of EPSP slopes normalized to control values recorded from six $Prnp^{0/0}$ slices from four mice (●) and five control slices from four mice (○). The two cases showed similar magnitudes and time courses of LTP.

ized reversal potential, the slope of the current–voltage relationship was lower in $Prnp^{0/0}$ mice (12, 13). This difference in conductance is determined largely by the stimulus strength and number of synapses activated and, therefore, says little about the underlying synaptic conductance.

We next studied the kinetics of monosynaptic IPSCs mediated by spontaneous or evoked activation of $GABA_A$ receptors using whole-cell voltage-clamp recordings in CA1 neurons. The presence of inhibitory synapses on the soma of pyramidal cells in the hippocampus provide a favorable situation for using voltage-clamp techniques to study the kinetics of the underlying inhibitory currents. We have therefore recorded IPSCs in neurons voltage-clamped at different membrane potentials. Using low-intensity stimulation, we found that decay of the stimulus-evoked IPSC is prolonged as the membrane potential is depolarized (Fig. 3*A* and *B*) (22, 23). However, no difference in the decay time constants of evoked IPSCs was observed between control and $Prnp^{0/0}$ mice (group II) at any membrane potential (Fig. 3*B*). The rise time was also measured for both the stimulus-evoked and spontaneous IPSCs (Fig. 3 *C* and *D*), and no difference was detected, contrary to a previous report (12). The slower rise time for the evoked IPSCs compared to the spontaneous IPSCs presumably reflects asynchrony in the release of GABA from the large number of synapses involved in generating the response.

In another set of experiments we examined whether LTP was altered in the $Prnp^{0/0}$ mice. During the experiments, we randomly interleaved, in a blind fashion, slices from control and $Prnp^{0/0}$ mice (group I). Only after the experiments had been fully analyzed and plotted was the code broken. The conditioning stimulus train was given at time 0 and reliably induced LTP lasting for at least 60 min. As can be seen in Fig. 4, no significant difference existed between the $Prnp^{0/0}$ and control animals, a finding that differs from recently published results in which LTP was reported to be impaired in $Prnp^{0/0}$ mice (12, 14).

Because genetic background can profoundly modify the phenotype of transgenic mice (24, 25), we have analyzed $Prnp^{0/0}$ animals from three different genetic backgrounds. However, no alteration was found in the excitability or the synaptic transmission of CA1 hippocampal pyramidal cells in all $Prnp^{0/0}$ mice. These results are consistent with previous

developmental and behavioral studies in which no abnormalities were found (11). In particular, they agree with results showing that synaptic transmission in cerebellar Purkinje cells and at the neuromuscular junction is normal in $Prnp^{0/0}$ mice (26, 27). However, they are in striking contrast to recent results, in which changes in $GABA_A$ receptor-mediated inhibition and LTP were reported in CA1 hippocampal pyramidal cells (12–14). It is possible that the differences observed between the $Prnp^{0/0}$ animals and the C57BL/6, 129/Sv, and (C57BL/6 × 129/Sv)F_1 controls is due to the genetic background of the $Prnp^{0/0}$ strain maintained by inbreeding (12–14). Indeed, some memory tasks have been shown to be strongly influenced by genetic background (28, 29). Further experiments will be needed to clarify this issue. Thus, the function of PrP^C in the normal hippocampus, where this protein is expressed at higher levels than many other regions of the central nervous system (30), remains enigmatic. Our results suggest that, whatever the role of PrP^C might be, its absence has little or no impact on the excitability of CA1 pyramidal cells as well as synaptic transmission and supports the hypothesis that it is the accumulation of PrP^{Sc} and not the loss of PrP^C that is responsible for the pathology in prion diseases (9, 15). If our findings in mice prove to be translatable to humans, then gene therapy aimed at reducing PrP expression may be a reasonable strategy in the treatment or prevention of the human prion diseases.

We thank Dr. G. A. Carlson and members from both Roger A. Nicoll and Stanley B. Prusiner's laboratories for their comments on the manuscript and Yin Qiu for helping us in obtaining the animals used for the study. This work was supported by National Institute of Mental Health (R.A.N.), National Institutes of Health, and American Health Assistance Foundation (S.J.D. and S.B.P.). P.-M.L. was supported by the Centre National de la Recherche Scientifique and by a North Atlantic Treaty Organization fellowship. R.A.N. is a member of the Keck Center for Integrative Neuroscience and the Silvio Conte Center for Neuroscience Research.

1. Gajdusek, D. C. (1977) *Science* **197,** 943–960.
2. Prusiner, S. B. (1991) *Science* **252,** 1515–1522.
3. Borchelt, D. R., Scott, M., Taraboulos, A., Stahl, N. & Prusiner, S. B. (1990) *J. Cell Biol.* **110,** 743–752.
4. Caughey, B. & Raymond, G. J. (1991) *J. Biol. Chem.* **266,** 18217–18223.
5. Pan, K.-M., Baldwin, M., Nguyen, J., Gasset, M., Serban, A., Groth, D., Mehlhorn, I., Huang, Z., Fletterick, R. J., Cohen, F. E. & Prusiner, S. B. (1993) *Proc. Natl. Acad. Sci. USA* **90,** 10962–10966.
6. Gabizon, R., McKinley, M. P., Groth, D. F. & Prusiner, S. B. (1988) *Proc. Natl. Acad. Sci. USA* **85,** 6617–6621.
7. Büeler, H., Aguzzi, A., Sailer, A., Greiner, R.-A., Autenried, P., Aguet, M. & Weissmann, C. (1993) *Cell* **73,** 1339–1347.
8. Prusiner, S. B., Groth, D., Serban, A., Stahl, N. & Gabizon, R. (1993) *Proc. Natl. Acad. Sci. USA* **90,** 2793–2797.
9. Prusiner, S. B. (1994) *Annu. Rev. Microbiol.* **48,** 655–685.
10. Prusiner, S. B. & DeArmond, S. J. (1994) *Annu. Rev. Neurosci.* **17,** 311–339.
11. Büeler, H., Fisher, M., Lang, Y., Bluethmann, H., Lipp, H.-P., DeArmond, S. J., Prusiner, S. B., Aguet, M. & Weissmann, C. (1992) *Nature (London)* **356,** 577–582.
12. Collinge, J., Whittington, M. A., Sidle, K. C. L., Smith, C. J., Palmer, M. S., Clarke, A. R. & Jefferys, J. G. R. (1994) *Nature (London)* **370,** 295–297.
13. Whittington, M. A., Sidle, K. C. L., Gowland, I., Meads, J., Hill, A. F., Palmer, M. S., Jefferys, J. G. R. & Collinge, J. (1995) *Nat. Genet.* **9,** 197–201.
14. Manson, J. C., Hope, J., Clarke, A. R., Johnston, A., Black, C. & MacLeod, N. (1995) *Neurodegeneration* **4,** 113–114.
15. Prusiner, S. B., Groth, D., Serban, A., Koehler, R., Foster, D., Torchia, M., Burton, D., Yang, S.-L. & DeArmond, S. J. (1993) *Proc. Natl. Acad. Sci. USA* **90,** 10608–10612.
16. Capecchi, M. R. (1989) *Trends Genet.* **5,** 70–76.
17. Doetschman, T., Maeda, N. & Smithies, O. (1988) *Proc. Natl. Acad. Sci. USA* **85,** 8583–8587.
18. Nicoll, R. A. & Alger, B. E. (1981) *J. Neurosci. Methods* **4,** 153–156.
19. Ben-Ari, Y., Cherubini, E., Corradetti, R. & Gaiarsa, J. L. (1989) *J. Physiol. (London)* **416,** 303–325.
20. Zhang, L., Spigelman, I. & Carlen, P. L. (1991) *J. Physiol. (London)* **444,** 25–49.
21. Blanton, M. G., Lo Turco, J. J. & Kriegstein, A. R. J. (1989) *Neurosci. Methods* **30,** 203–210.
22. Gray, R. & Johnston, D. J. (1985) *Neurophysiology* **54,** 134–142.
23. Collingridge, G. L., Gage, P. W. & Robertson, B. (1984) *J. Physiol. (London)* **356,** 551–564.
24. Sibilia, M. & Wagner, E. F. (1995) *Science* **269,** 234–238.
25. Threadgill, D. W., Dlugosz, A. A., Hansen, L. A., Tennenbaum, T., Lichti, U., Yee, D., LaMantia, C., Mourton, T., Herrup, K., Harris, R. C., Barnard, J. A., Yuspa, S. H., Coffey, R. J. & Magnuson, T. (1995) *Science* **269,** 230–234.
26. Herms, J. W., Kretzschmar, H. A., Titz, S. & Keller, B. U. (1995) *Eur. J. Neurosci.* **7,** 2508–2512.
27. Brenner, H. R., Herczeg, A. & Oesch, B. (1992) *Proc. R. Soc. London B* **250,** 151–155.
28. Paylor, R., Baskall, L. & Wehner, J. M. (1993) *Psychobiology* **21,** 11–26.
29. Bowers, B. J., Christensen, S., Pauley, J. R., Yuva, L., Dunbar, S. E. & Wehner, J. M. (1995) *J. Neurochem.* **64,** 2737–2746.
30. DeArmond, S. J., Mobley, W. C., DeMott, D. L., Barry, R. A., Beckstead, J. H. & Prusiner, S. B. (1987) *Neurology* **37,** 1271–1280.